Drug Design, Development and Therapy

Dovepress

open access to scientific and medical research

Open Access Full Text Article

ORIGINAL RESEARCH

Cardioprotective Effect of Monoammonium Glycyrrhizinate Injection Against Myocardial Ischemic Injury in vivo and in vitro: Involvement of Inhibiting Oxidative Stress and Regulating Ca^{2+} Homeostasis by L-Type Calcium Channels

This article was published in the following Dove Press journal:
Drug Design, Development and Therapy

Zhifeng Zhao,[1,*] Miaomiao Liu,[1,*] Yuanyuan Zhang,[1] Yingran Liang,[1] Donglai Ma,[1] Hongfang Wang,[1] Zhihong Ma,[2] Shengjiang Guan,[2] Zhonglin Wu,[3] Xi Chu,[3] Yue Lin,[2] Li Chu[1,4]

[1]School of Pharmacy, Hebei University of Chinese Medicine, Shijiazhuang 050200, Hebei, People's Republic of China; [2]School of Basic Medicine, Hebei University of Chinese Medicine, Shijiazhuang 050200, Hebei, People's Republic of China; [3]The Fourth Hospital of Hebei Medical University, Shijiazhuang 050011, Hebei, People's Republic of China; [4]Hebei Key Laboratory of Integrative Medicine on Liver-Kidney Patterns, Shijiazhuang 050200, Hebei, People's Republic of China

*These authors contributed equally to this work

Correspondence: Li Chu
School of Pharmacy, Hebei University of Chinese Medicine, Shijiazhuang 050200, Hebei, People's Republic of China
Email chuli0614@126.com

Yue Lin
School of Basic Medicine, Hebei University of Chinese Medicine, Shijiazhuang 050200, Hebei, People's Republic of China
Tel/Fax +86 311 89926718
Email yuelin8992@126.com

Purpose: Monoammonium glycyrrhizinate (MAG) is an aglycone of glycyrrhizin that is found in licorice and is often used clinically as an injection to treat liver diseases. However, the effect of MAG injection on cardiac function and its possible cellular mechanisms remain unclear. We explored the protective effects of MAG against myocardial ischemic injury (MII) induced by isoproterenol (ISO), as well as the cellular mechanisms via molecular biology techniques and patch-clamp recording.

Methods: A rat model of myocardial ischemia injury was induced by administering ISO (85 mg/kg) subcutaneously for 2 consecutive days. ECG, cardiac functional parameters, CK and LDH levels, SOD and GSH activities, MDA concentration, histological myocardium inspection, mitochondria ultrastructure changes, intracellular calcium concentrations were observed. Influences of MAG on $I_{Ca\text{-}L}$ and contraction in isolated rat myocytes were observed by the patch-clamp technique.

Results: MAG reduced damage, improved cardiac morphology, inhibited oxidative stress, decreased the generation of reactive oxygen species, and decreased intracellular Ca^{2+} concentration. Exposure of the rats' ventricular myocytes to MAG resulted in a concentration-dependent reduction in L-type calcium currents ($I_{Ca\text{-}L}$). MAG reduced $I_{Ca\text{-}L}$ in a consistent and time-dependent fashion with a semi-maximal prohibitive concentration of MAG of 14 μM. MAG also shifted the I-V curve of $I_{Ca\text{-}L}$ upwards and moved the activation and inactivation curves of $I_{Ca\text{-}L}$ to the left.

Conclusion: The findings indicate that MAG injection exerts a protective influence on ISO-induced MII by inhibiting oxidative stress and regulating Ca^{2+} homeostasis by $I_{Ca\text{-}L}$.

Keywords: cardiopretection, reactive oxygen species, calcium influx, isoproterenol, calcium concentration

Introduction

Licorice is used as an herbal medicine and is native to East Asia and Southern Europe. It has beneficial applications in both medicine and confections[1] and is obtained from *Glycyrrhiza uralensis* Fisch (*Glycyrrhiza glabra* L.).[2] Monoammonium glycyrrhizinate (MAG) (Figure 1) is an aglycone of glycyrrhizin that is derived from licorice, and modern medical research has shown that this substance is the main bioactive

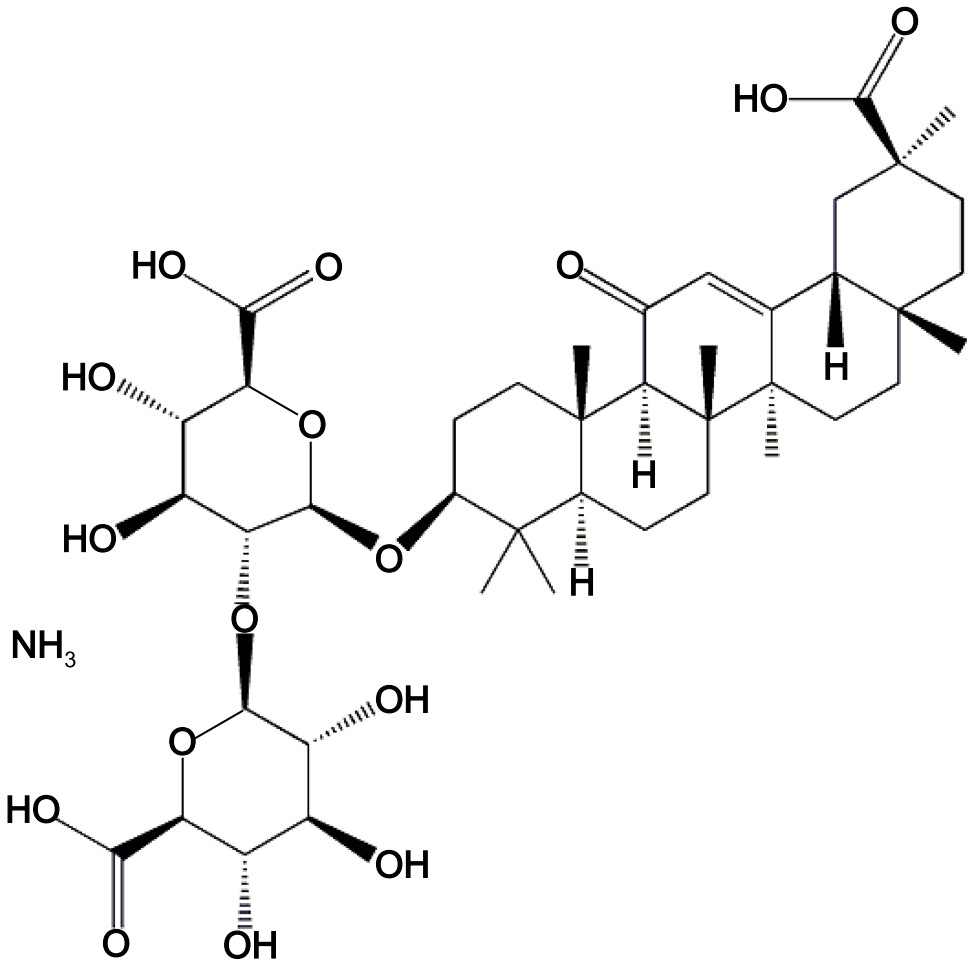

Figure 1 Chemical structure of MAG.

component of the plant. Many studies have focused on glycyrrhizic acid and its derivatives, which have many biological functions,[3,4] such as liver detoxification effects[5,6] and antiallergic activities.[7,8] MAG has also been used clinically as an injection to treat liver diseases.[9,10]

Oxidative stress is a process that causes oxidative damage through imbalance between the production and elimination of oxygen free radicals in the body or cells, which results in the accumulation of reactive oxygen species (ROS).[11] In great quantities, free radicals can cause tissue and cell damage through a series of peroxidation reactions. Changes in malondialdehyde (MDA), a lipid peroxidation product, can indirectly reflect the metabolism of oxygen free radicals in vivo, and its level reflects the severity of free radical attack on cells.[12]

Superoxide dismutase (SOD) is a specific scavenger that has great significance in the activities of the body. As an important scavenger of oxygen free radicals in vivo, it is an important antioxidant enzyme and can protect cells from damage. The level of SOD can indirectly reflect the ability of the body to remove free radicals.[13] The production and removal of free radicals occur in a dynamic equilibrium state so that they do not easily cause tissue damage.

The interaction of free radicals and membrane-lipid unsaturated fatty acids leads to lipid peroxidation, which causes an imbalance in the ratio of membrane unsaturated fatty acid to protein.[14] This interaction also decreases the liquidity, fluidity, and permeability of cell membranes and organelle membranes, increases the influx of Ca^{2+} and indirectly inhibits the function of membrane protein. These phenomena lead to increased concentrations of cytoplasmic Ca^{2+} cell swelling, and calcium overload.[15]

Isoproterenol (ISO) is a synthetic catecholamine, and its administration causes severe stress in the myocardium due to the activation of the adrenergic system and other neurohumoral systems, which lead to increases in L-type Ca^{2+} channel (LTCC) activity.[16] Ischemic heart disease (IHD) is the most widely cited reason for morbidity and

disability in the modern world. Heart failure, hypertension, and ischemia from atherosclerosis partly result from changes in intracellular Ca^{2+} Mitochondrial permeability transition pores (mPTPs) may be involved in the release of mitochondrial components during cell death and play an important role in cell survival and apoptosis.[17] Calcium overload might lead to the opening of mPTPs, plasmalemma rupture, and even cell death.[15] LTCCs are the main path of influx for Ca^{2+} and are important for the treatment of ischemic cardiac disease.[18]

MAG injection has anti-inflammatory, anti-allergic, and membrane-protective effects. Thus, it has been used clinically for immunoregulation, the promotion of bilirubin metabolism, the inhibition of viral hepatitis, the improvement of liver function, and as an adjuvant treatment for radiotherapy and chemotherapy when treating cancer.[10] However, the cardioprotective effects of MAG injection have not been proven. We speculate that MAG exerts a myocardial protective effect by improving oxidative stress and reducing cytoplasmic Ca^{2+} concentration by LTCCs.

In the present study, we evaluated the effects of MAG injection on LTCC current ($I_{Ca\text{-}L}$) in myocardial cells from rats to elaborate the underlying cellular mechanisms of its protective effects against myocardial ischemic injury (MII). To this end, we examined the oxidative response by the production of ROS, MDA, and SOD, detected changes in cytoplasmic Ca^{2+} concentration, and used patch-clamp techniques to study the influence of MAG injection. The findings could contribute to efforts to improve the efficacy of MAG injection in clinical treatments.

Materials and Methods

Materials

MAG injections were purchased from Yuanye Bio-Technology Co., Ltd. (Shanghai, China). ISO was purchased from Amylet Scientific Inc. (Michigan, USA). Verapamil (Ver) was purchased from HeFeng Pharmaceutical Co., Ltd. (Shanghai, China). Other reagents were purchased from Sigma-Aldrich (St. Louis, MO, USA). Every solvent used in the experiments was of analytical purity.

Animals

Male adult Sprague-Dawley rats were purchased from the Experimental Animal Center of Hebei Medical University and housed in standard growth conditions (20–24 degrees celsius, 40–60% relative humidity, 12-h light-dark cycle). The experiments began after at least a 7 days of adaptation to the laboratory environment. All experimental and animal handling procedures were approved by the Ethics Committee for Animal Experiments of Hebei University of Chinese Medicine (approval number: DWLL2018028; approval date: December 20, 2018) and conformed to the National Institutes of Health Guidelines for the Care and Use of Laboratory Animals.

Induction of MII

Forty adult male SD rats (200–240 g) were kept at 20–24 degrees celsius, with free intake of water and food. After 1 week of adaptive feeding, all animals were randomly allocated to a control (Con), ISO, MAG, or verapamil (Ver) group (n = 10 in each group). The MAG group and Ver group were respectively given MAG (30 mg/kg/d) and Ver (2 mg/kg/d), while the Con group and ISO group were injected with purified water. All injections were intraperitoneal. After 1 week of continuous treatment with these methods, ISO was injected subcutaneously (85 mg/kg) for two consecutive days in all groups except for the Con group. All experiments were approved by the Ethics Committee of Hebei University of Chinese Medicine.

Acquisition of Electrocardiogram (ECG) and Cardiac Functional Parameters

ECG recordings of J-point elevation and heart rate were obtained from the animals using a BL-420S biological function experimental system. Anesthesia was performed by intraperitoneal injection of ethyl carbamate (1.0 g/kg), and ECG was performed at 30 min after the last injection of ISO or a placebo. Three needle electrodes were connected to the left front leg and both hind legs of the animals.

Catheterization of the left ventricle (LV) was performed on anesthetized rats after finishing the final injection of ISO. A miniature pressure transducer (Chengdu instrument Co., Chengdu, China) was inserted into the LV via the right carotid artery and advanced into the LV under continuous monitoring of the pressure waveform. Pressure signals were digitized and recorded with the BL-420S. The heart rate (HR), left ventricular systolic pressure (LVSP), left ventricular diastolic pressure (LVDP), and the first derivatives of left intraventricular pressure (rate of pressure development $+dP/dt_{max}$ and rate of pressure decrease $-dP/dt_{max}$) were monitored continuously, recorded, and analyzed after 10 min of stabilization.

Detection of CK and LDH Activities

The sera of rats were separated by centrifugation, and the levels of diagnostic marker enzymes CK and LDH in serum were determined using standard commercial kits (JianCheng, Nanjing, China).

Detection of SOD, Glutathione (GSH) Activities, and MDA Concentration

The sera were separated by centrifugation. The SOD activity, GSH activity, and MDA concentration were measured using standard commercial kits (Nanjing Jiancheng Bioengineering Institute, JianCheng, Nanjing, China) according to the manufacturer's instructions. For the preparation of myocardial tissue, a well-ground 10% homogenate of heart tissue was centrifuged at 3000 r/min for 10–15 min at low temperature to prepare a supernatant for the determination of biochemical indicators. The heart tissue homogenate was used to evaluate SOD and GSH activities and the concentration of MDA using commercial kits (Jiancheng, Nanjing, China).

Histological Inspection of Myocardium

Rat hearts were extracted rapidly after sacrificing the animals and fixed in 4% paraformaldehyde. The hearts were then cleared, dehydrated, made transparent, impregnated, and embedded in paraffin. Hematoxylin-eosin (H&E) staining was performed on 5-μm-thick sections.

Ultrastructural Examination of Mitochondria

Cardiac tissue was excised, trimmed to 1 mm^3, and fixed in 2.5% glutaraldehyde in 0.1 M sodium phosphate buffer at pH 7.4 and 4°C for 3 h. Next, it was osmicated in 1% osmium tetroxide for 1 h at 4°C and prepared for thin sectioning. After dehydration with a graded ethanol series, the thin sections were observed and photographed with a transmission electron microscope (TEM) at 80 kV (7650 TEM, Hitachi, Tokyo, Japan).

Detection of Intracellular ROS

The fluorescence of a dihydroethidium probe (DHE, Cat. Beyotime Institute of Biotechnology, Shanghai, China) was used to analyze the ROS generation in cardiac tissues. The ROS production was labeled with red fluorescence, which was visualized and evaluated using high content.

Detection of Intracellular Calcium Concentration

The calcium concentration was determined in myocardial tissue and free cardiomyocytes. Heart tissue samples were homogenized in a 10% (W/V) buffered solution. The homogenate was centrifuged (1000 rpm, 10 min), and the upper clear liquid was used for all downstream biochemical analyses. The calcium level was assessed by Coomassie Brilliant Blue staining with a commercial kit (Jian Cheng, Nanjing, China).

Cardiomyocytes were isolated as described below. Experiments were performed to measure the fluorescence of Cardiomyocytes (CAF-100, Japan Spectroscopic, Tokyo, Japan). At the beginning of the experiments, cells in suspension were equilibrated for 2–3 min before data collection and incubated with 2 μM fura-2/AM for 30 min at 37°C. The excitation wavelength alternated between 340 and 380 nm at intervals of 1 s with the emission wavelength set at 510 nm. The plateau levels of the intracellular free calcium concentration were used for analysis. The intracellular free calcium concentration was calculated using a described previously equation.[19]

Isolation of Cardiomyocytes

To obtain normal cardiomyocytes, single ventricular myocardial cells were isolated from animals that had been tranquilized via intraperitoneal injections of heparin sodium (500 IU/kg) and sodium pentobarbital (40 mg/kg). The heart was quickly cut out of the animal and canulated on a Langendorff instrument for perfusion with an oxygenated frostbound free calcium Tyrode's solution. The solution contained 5.4 mM KCl, 135 mM NaCl, 0.33 mM NaH_2PO_4, 1.0 mM $MgCl_2$, 10 mM glucose, and 10 mM HEPES. The pH was adjusted to 7.4 using 3 M NaOH. Next, the heart was perfused with an enzymatic solution containing Ca^{2+}-free Tyrode's solution with 30 μmol/L of $CaCl_2$, 0.6 mg/mL of collagenase type II, and 0.5 mg/mL of bovine serum albumin. After perfusion, the cardiac tissue was decomposed into fragments in Kreb's buffer solution. The cardiomyocytes were kept in Kreb's buffer solution for up to 1 h before subsequent experiments.

To obtain ischemic cardiomyocytes, ISO (85 mg/kg) was subcutaneously injected into rats to induce myocardial ischemia. The dosages and paradigms of injections were performed according to previous studies.[20] After induction of myocardial ischemia for two consecutive days, the heart

was removed and used for the same experiments as the normal rat ventricular myocytes.

Electrical Recordings of L-Type Ca^{2+} Currents

LTCC expression on ventricular myocytes was measured by the whole cell patch clamp technique. A pipette puller (Sutter Instruments, Novato, California, USA) was used to pull borosilicate glass electrodes. $I_{Ca\text{-}L}$ was recorded using an Axon Patch 200B amplifier, and pCLAMP10.0 software was used for analysis (Axon Instruments, Union City, CA, USA). The currents were screened at 2 kHz.

Statistical Analysis

The data obtained were expressed as the mean ± standard error of the mean (SEM) and were analyzed by one-way analysis of variance (ANOVA), followed by a Student's *t*-test using Origin Pro 9.1 software. $P < 0.05$ was considered as statistically significant.

Results

Actions of MAG on Electrocardiography and Cardiac Functional Parameters

Compared with the Con group (Figure 2), the heart rate and J-point elevation were dramatically elevated in animals with ISO-induced MII ($p < 0.05$ or $p < 0.01$). This shows that the MII model was successfully established. A marked decrease in these two indicators ($p < 0.05$ or $p < 0.01$) occurred in the MAG group in comparison to the ISO group.

Heart rate, LVEDP, and $\pm dp/dt_{max}$ in ISO-treated animals were compared to those in the control group. Table 1 shows that the pretreatment of rats with MAG

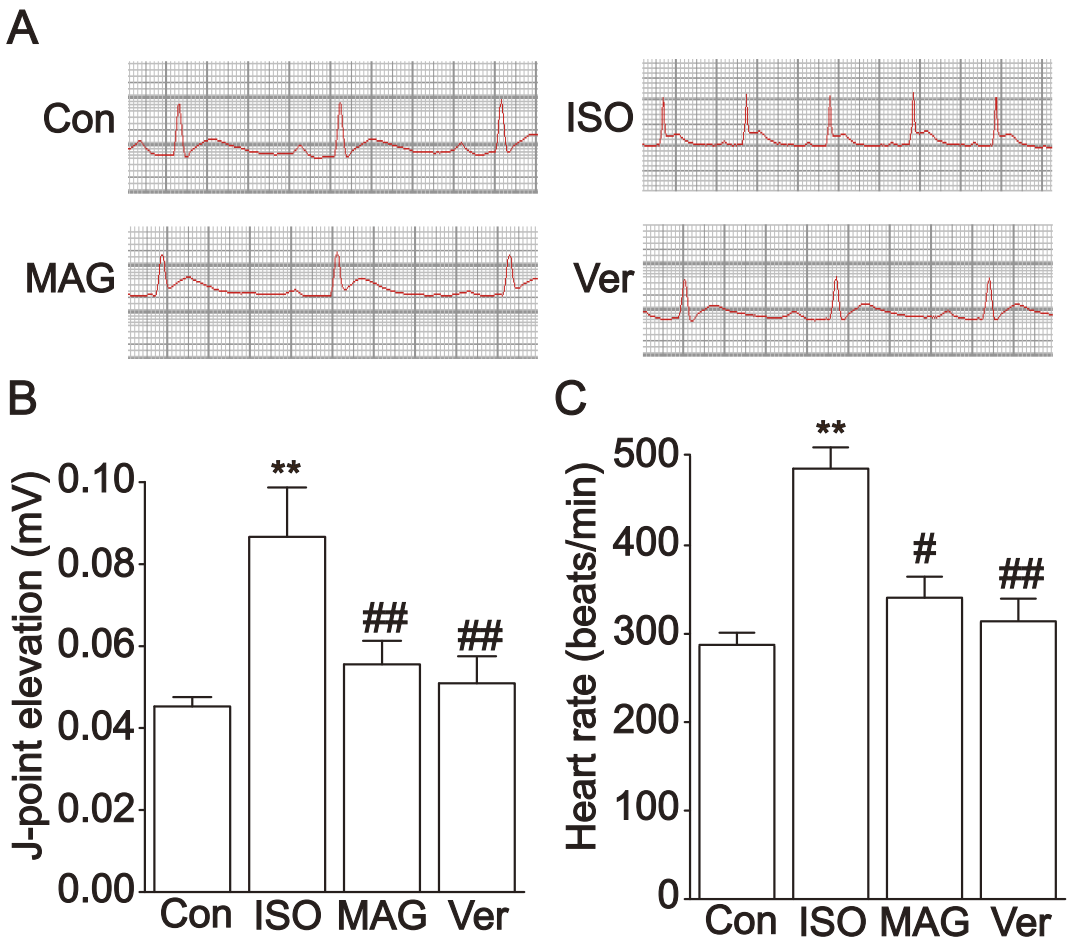

Figure 2 Actions of MAG on ECG. Representative ECG tracings of each group (**A**). Statistical analysis of J-point elevation (**B**) and heart rate (**C**) in each group. The values are the mean ± standard deviation (n=10). Compared to the Con group (**p<0.01); Compared to the ISO group ($^{\#}p$<0.05); Compared to the ISO group ($^{\#\#}p$<0.01).

Table 1 Effects of MAG on Changes of Cardiac Functional Parameters

Group	LVEDP (mmHg)	LVSP (mmHg)	+dp/dt$_{max}$ (mmHg/s)	-dp/dt$_{max}$ (mmHg/s)
Con	5.4 ± 0.68	151.9 ± 17.11	6143.7 ± 761.91	5611.1 ± 710.48
ISO	20.5 ± 1.81**	107.1 ± 14.05**	3743.6 ± 451.29**	3343.8 ± 420.29**
MAG	14.9 ± 1.67$^{\#}$	126.5 ± 16.34$^{\#}$	5230.1 ± 549.71$^{\#\#}$	4930.6 ± 590.71$^{\#\#}$
Ver	9.7 ± 0.76$^{\#\#}$	139.2 ± 18.62$^{\#}$	5822.7 ± 690.06$^{\#\#}$	5122.8 ± 621.37$^{\#\#}$

Notes: Values are means ± SEM (n=10). **p<0.01 vs Con group. $^{\#}p$<0.05 vs ISO group; $^{\#\#}p$<0.01 vs ISO group.

and Ver caused restoration of both parameters to nearly normal levels. Before the injection of ISO, the groups pretreated with MAG and Ver showed no significant difference from the control and ISO group ($p < 0.05$ or $p < 0.01$).

Effects of MAG on CK and LDH Activities

MII was appraised by detecting CK and LDH activities (Figure 3). An obvious elevation was measured in the activities of CK and LDH in the ISO group in comparison with the Con group ($p < 0.01$). Nevertheless, there was an obvious reduction in the MAG and Ver groups in comparison with the ISO group ($p < 0.05$ or $p < 0.01$).

Effects of MAG on SOD, GSH Activities, and MDA Levels

The oxidative stress response was evaluated by detecting the activity of SOD, GSH, and MDA levels (Figures 4 and 5). In the serum experiment, the ISO group had obviously higher MDA levels than the Con group, but SOD and GSH activity decreased ($p < 0.01$), as shown in Figure 4. The MDA levels decreased in the MAG and Ver groups after treatment, while the SOD and GSH activities increased ($p < 0.01$, $p < 0.05$).

In experiments measuring oxidative stress in myocardial tissue, the ISO group had obviously increased MDA levels compared to the Con group, but SOD and GSH activity decreased ($p < 0.01$), as shown in Figure 5. The MDA levels decreased in the MAG and Ver groups, but the SOD and GSH activities increased ($p < 0.01$, $p < 0.05$).

Actions of MAG on Histopathology

Figure 6A–D show the histopathology changes in the rat hearts detected by light microscopy. Natural muscle fibril structure was detected in the cardiac organization slices in the Con group (Figure 6A), whereas the ISO group demonstrated cardiomyocyte swelling, vestigial infiltrating inflammatory cells, and the disappearance of transverse striations (Figure 6B). The MAG and Ver groups showed similarly normal structures with clear transverse fringes, as well as slight edema and a small amount of inflammatory cardiomyocytes in comparison to the ISO group (Figure 6C and D).

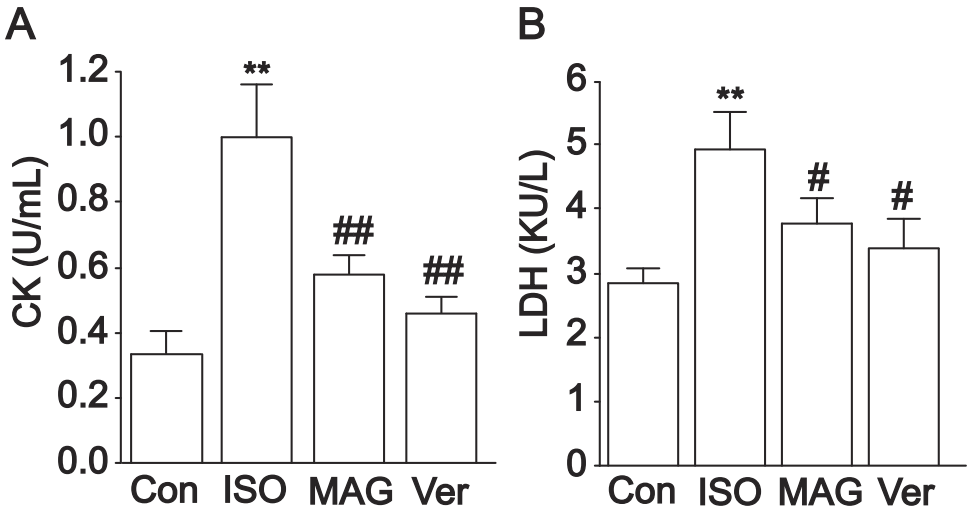

Figure 3 Actions of MAG on cardiac markers. The activities of CK (**A**) and LDH (**B**) were determined. The values are the mean ± standard deviation (n=10). Compared to the Con group (**p<0.01); Compared to the ISO group ($^{\#}p$<0.05); Compared to the ISO group ($^{\#\#}p$<0.01).

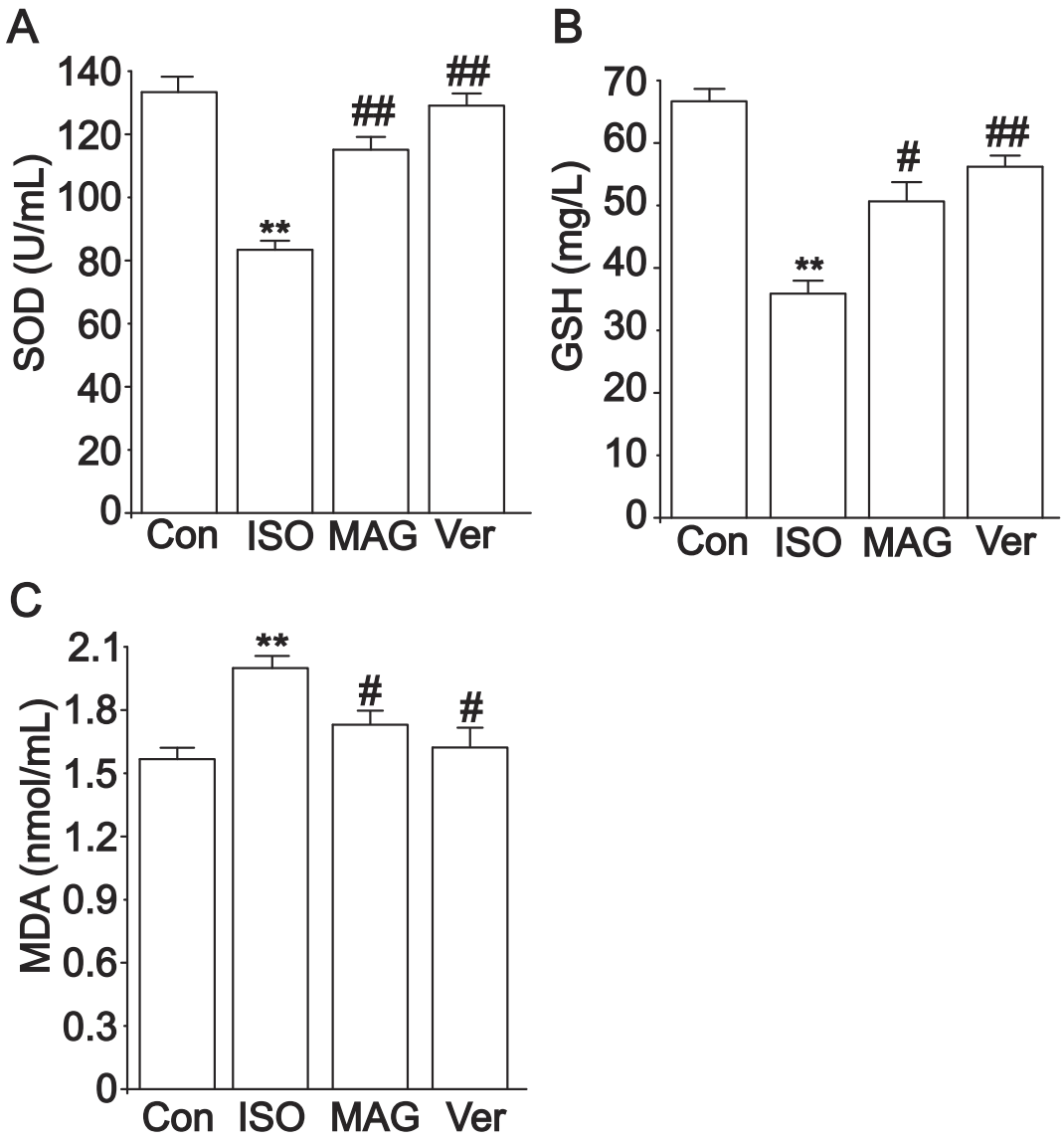

Figure 4 Actions of MAG on the activities of SOD (**A**), GSH (**B**), and MDA (**C**) levels in serum. The values are the mean ± standard deviation (n=10). Compared to the Con group ($^{**}p< 0.01$); Compared to the ISO group ($^{\#}p<0.05$); Compared to the ISO group ($^{\#\#}p<0.01$).

Actions of MAG on the Myocardial Mitochondrion Ultrastructure

As shown in Figure 6, the mitochondrial ultrastructures were observed by TEM. Cardiomyocytes of the control animals exhibited regularly shaped cylinders composed of Z lines with dyads, sarcomeres, elliptical nuclei, numerous mitochondria, and prominent myofilaments (Figure 6E). Compared to the Con group, the ISO group showed distinctive ultrastructure alterations. Edema was evident, and sarcomeres and myofilament arrangements were disordered and partially separated. The mitochondria were enlarged and rounded, and the cristae appeared disordered or disrupted (Figure 6F). However, the damage to myocardial ultrastructures in the MAG-treated and Ver-treated groups was attenuated compared with that of the ISO group (Figure 6G and H).

Effects of MAG on ROS Release

Figure 7A shows the ROS of rat heart tissue according to the DHE fluorescent probe analysis. MAG and Ver obviously reduced the production of ROS in cardiomyocytes. As shown in Figure 7A, the intracellular ROS levels were higher in the ISO group than the Con group ($p < 0.01$). Figure 7B shows that the production of ROS in the ISO group was obviously increased compared to the Con group, and MAG and Ver evidently reduced the production of ROS in cardiomyocytes ($p < 0.01$).

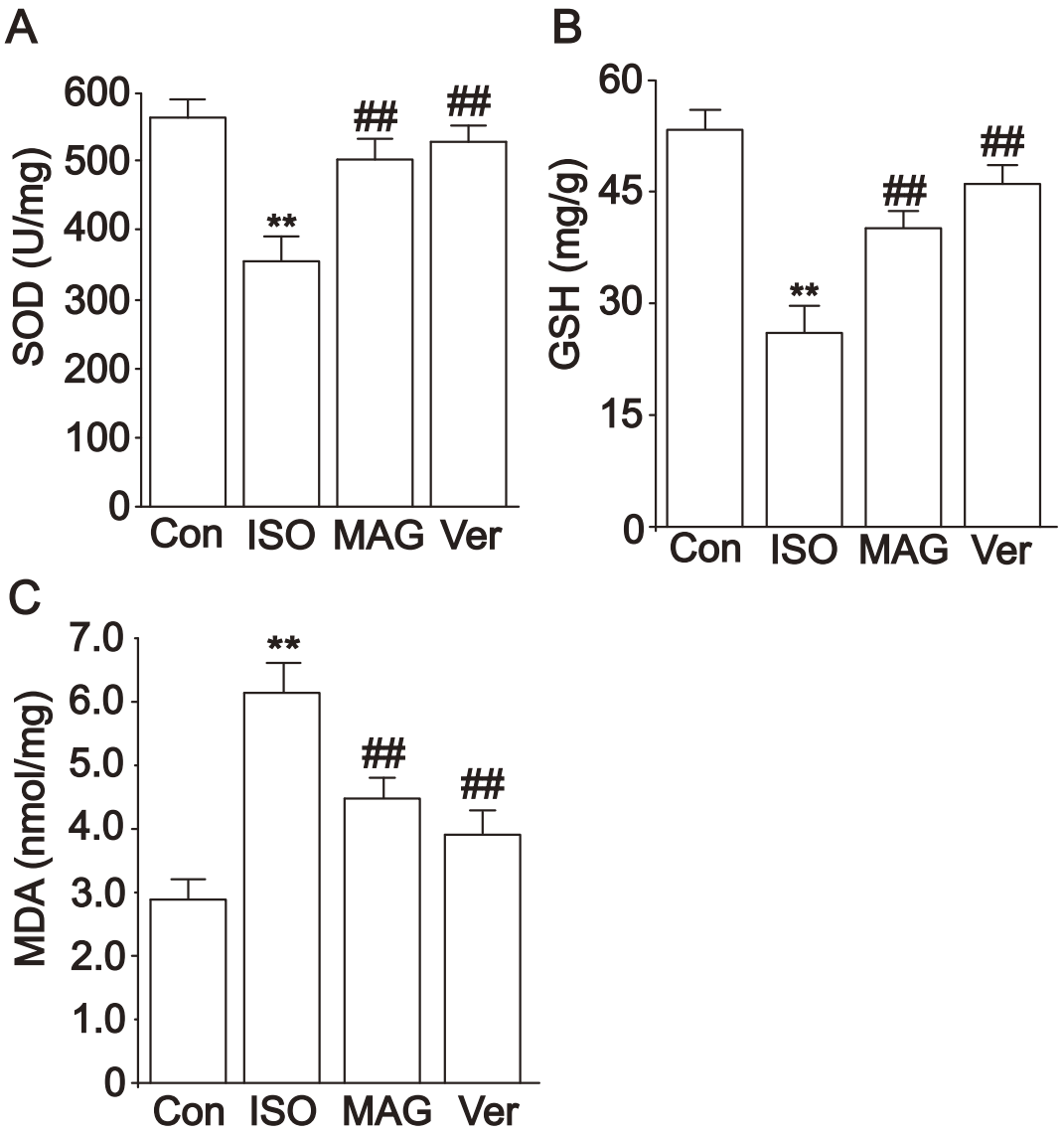

Figure 5 Actions of MAG on the activities of SOD (**A**), GSH (**B**), and MDA (**C**) levels in heart tissue. The values are the mean ± standard deviation (n=10). Compared to the Con group (**p< 0.01); Compared to the ISO group (##p<0.01).

Effects of MAG on Calcium Concentration

As shown in Figure 8A, calcium concentrations in the myocardial tissue of the ISO group increased significantly ($p < 0.01$) compared to the Con group, but they significantly decreased in the MAG group ($p < 0.01$) and Ver group ($p < 0.01$) in comparison to the ISO group. In the case of free cardiomyocytes, the ISO group had obviously increased calcium concentrations ($p < 0.01$) compared with the Con group, as shown in Figure 8B. However, the MAG group ($p < 0.01$) and Ver group ($p < 0.01$) showed significant decreases.

Determination of $I_{Ca\text{-}L}$

The $I_{Ca\text{-}L}$ was determined by the steady-state activation protocol. The application of Ver (0.1 mM), a specific L-type Ca^{2+} channel antagonist, nearly entirely blocked the currents (Figure 9) ($p < 0.01$). This indicates that these currents were L-type Ca^{2+} currents.

Inhibitory Effects of MAG on $I_{Ca\text{-}L}$

Healthy cardiomyocytes and ischemic cardiomyocytes were exposed to 1×10^{-4} M MAG, and the height of the $I_{Ca\text{-}L}$ peak decreased in both cases ($p < 0.01$). $I_{Ca\text{-}L}$ remained stable after washing with an external solution. Figure 10A, C and E show that MAG can inhibit $I_{Ca\text{-}L}$ in healthy cardiomyocytes. Figure 10B, D and F show that MAG can inhibit $I_{Ca\text{-}L}$ in ischemic cardiomyocytes and that this inhibition is irreversible.

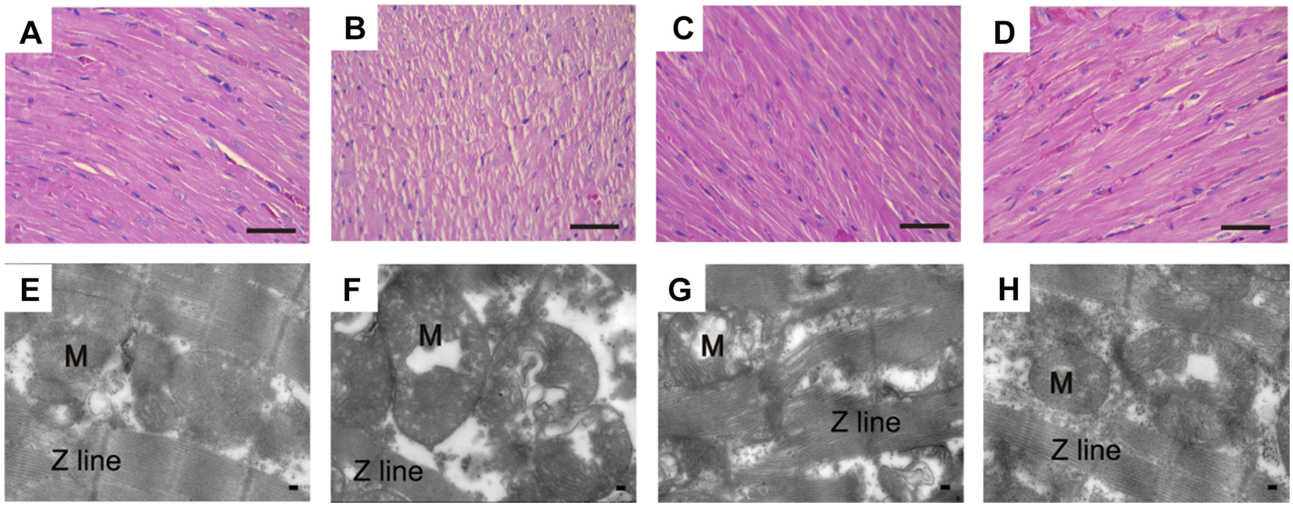

Figure 6 Actions of MAG on histopathological changes of animals' cardiac tissue colored with H&E and ultrastructural changes. Representative sections (magnification: 400×) were from the heart of the Con (**A**), ISO (**B**), MAG (**C**), and Ver (**D**) groups. Scale bar: 50 μm. The ultrastructure of heart tissues was detected by Transmission Electron Microscope (magnification: 15,000×) from the left ventricle of the Con (**E**), ISO (**F**), MAG (**G**), and Ver (**H**) groups. Scale bar: 1.0 μm.

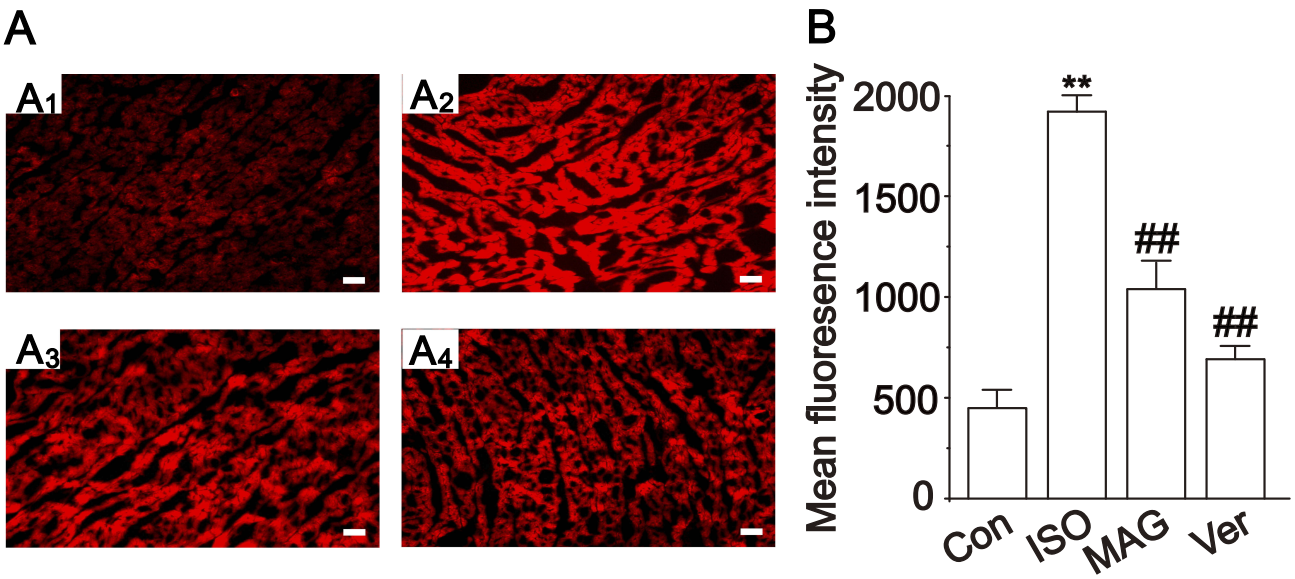

Figure 7 Actions of MAG on reactive oxygen species in rat heart tissue by fluorescent probe DHE. Representative sections are from the heart of the Con (A_1), ISO (A_2), MAG (A_3), and Ver (A_4) groups. Representative sections are from semi-quantitative calculation of ROS content in rat myocardium (**B**). The values are the mean ± standard deviation. Compared to the Con group ($^{**}p<0.01$); Compared to the ISO group ($^{\#\#}p<0.01$). Scale bar: 50 μm.

Dose Dependence of MAG on $I_{Ca\text{-}L}$

Figure 11 demonstrates the current traces obtained by depolarization with test potentials of −80 to 0 mV at various MAG concentrations. $I_{Ca\text{-}L}$ was gradually inhibited by raising concentrations of MAG from 10^{-6} to 10^{-4} M. The peak amplitudes of $I_{Ca\text{-}L}$ were reduced by 11.46 ± 0.80%, 18.76 ± 0.81%, 29.19 ± 2.10%, 45.33 ± 0.63%, and 54.32 ± 2.53%. MAG progressively suppressed $I_{Ca\text{-}L}$ in a dose-dependent manner. The semi-maximal prohibitive concentration of MAG was calculated as 14 μM.

Actions of MAG on the Current-Voltage Relationship of $I_{Ca\text{-}L}$

Figure 12 shows the effects of MAG (10^{-6}, $10,^{-5}$ 10^{-4} M) on the current-voltage relationship of $I_{Ca\text{-}L}$. Figure 12A shows cross-sectional traces with sequential treatments of 10^{-6}, 10^{-5} and 10^{-4} M of MAG. Figure 12B exhibits the current-density-voltage relationship with controls for 10^{-6}, 10^{-5} and 10^{-4} M of MAG and 10 μM of Ver. These results indicate that the different MAG concentrations significantly decreased the maximum current.

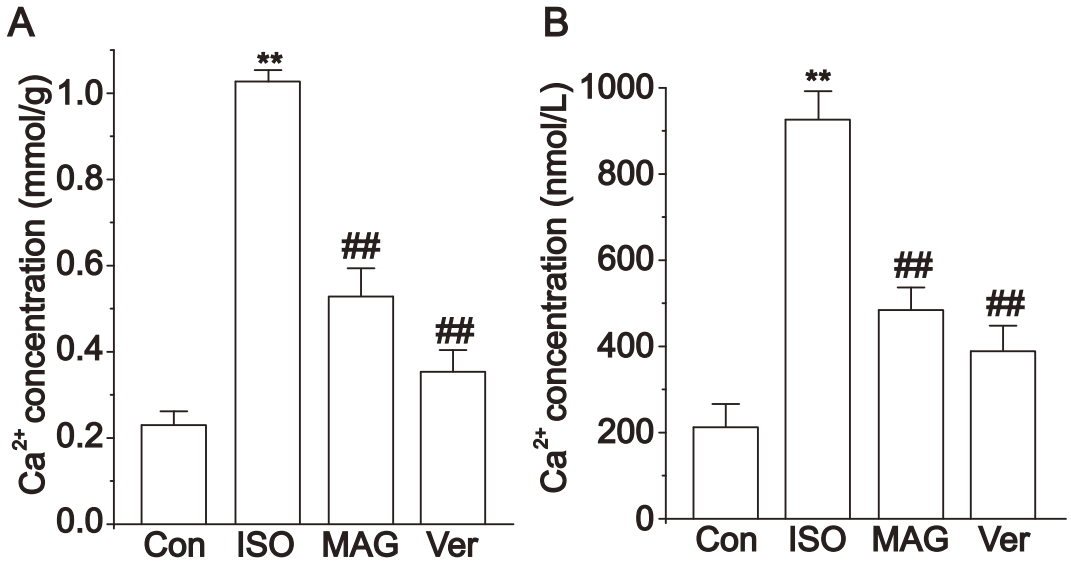

Figure 8 Actions of MAG on Ca^{2+} concentrations levels. (**A**) Calcium content in myocardial tissue homogenate. (**B**) Intracellular Ca^{2+} concentration in isolated ventricular myocytes with fluorescence spectrophotometer. The values are the mean ± standard deviation (n=10). Compared to the Con group (**p<0.01); Compared to the ISO group (##p<0.01).

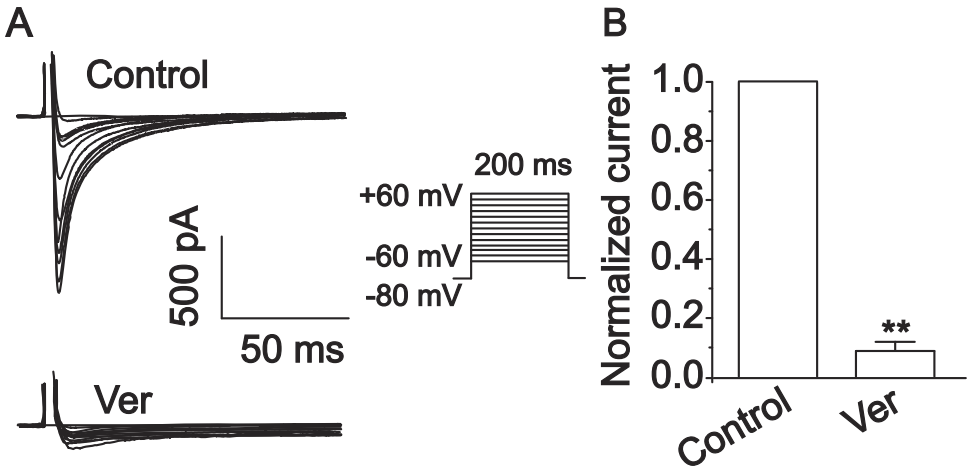

Figure 9 Ver (0.1 mM) wholly suppressed the Ca^{2+} current in cardiomyocytes. (**A**) Typical traces under verapamil treatment. (**B**) Summary data of A. The values are the mean±standard deviation (n=10 cells). **p<0.01 compared with Con.

Steady Activation and Inactivation of Ca^{2+} Current by MAG

Figure 13 presents the dependence of the steady-state activation and inactivation of Ca^{2+} current in the presence and absence of MAG (10^{-6}, $10,^{-5}$ and 10^{-4} M). The $V_{1/2}$ value of the normalized activation conductivity curve was −10.59 ± 0.74 mV, and the slope (k) of the control group was 7.67 ± 0.68 mV. The other $V_{1/2}$ values were −12.95 ± 0.59 mV (k = 7.27 ± 0.53 mV) for 10^{-6} mol/L of MAG, −12.37 ± 0.44 mV (k = 7.43 ± 0.40 mV) for 10^{-5} mol/L MAG, and −14.18 ± 0.51 mV (k = 7.12 ± 0.46 mV) for 10^{-4} mol/L of MAG.

The $V_{1/2}$ values of the steady-state inactivation were −30.55 ± 0.74 mV (k = 5.16 ± 0.72 mV) for the control, −33.25 ± 0.45 mV (k = 5.11 ± 0.40 mV) for 10^{-6} mol/L of MAG, −34.38 ± 0.40 mV (k = 5.19 ± 0.34 mV) for 10^{-5} mol/L of MAG, and −35.25 ± 0.23 mV (k = 5.27 ± 0.20 mV) for 10^{-4} mol/L of MAG. The results indicate that MAG did not change the activation and inactivation of gated characteristics of LTCC ($p > 0.05$). With or without MAG, there was no significant difference in the normal activation and inactivation values of $V_{1/2}$ ($p > 0.05$).

Discussion

IHD is a major type of cardiovascular disease, particularly myocardial infarction. The cellular mechanisms underlying the ISO-induced MII or hypoxia in the MII model

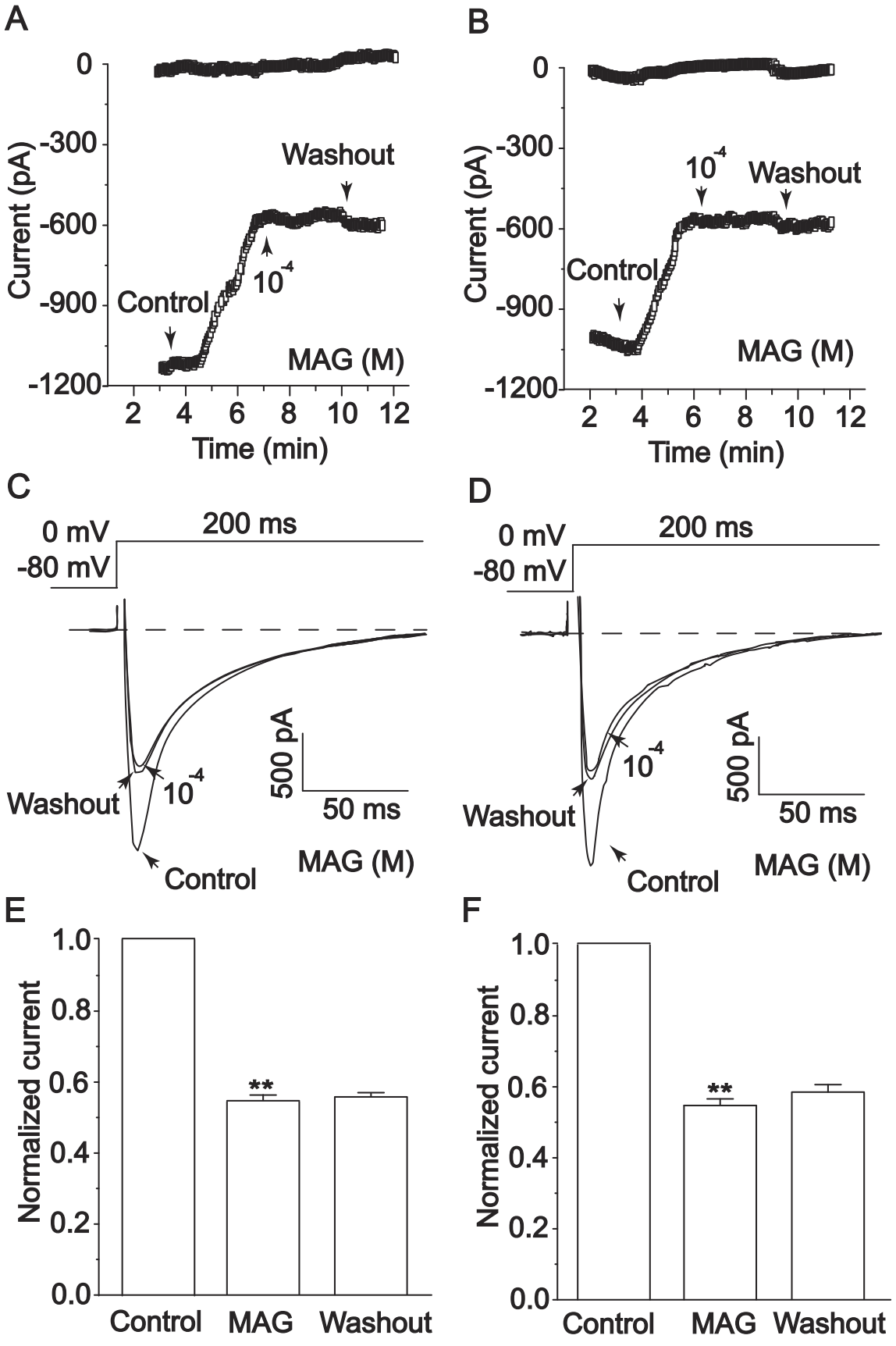

Figure 10 Actions of MAG on $I_{Ca\text{-}L}$ of healthy cardiomyocytes (**A,C,E**) and ischemic cardiomyocytes (**B,D,F**). MAG $I_{Ca\text{-}L}$ under control conditions, 1×10^{-4} M MAG, and washout. The values are the mean ± standard deviation (n=10 cells). $^{**}p<0.01$ compared with Con.

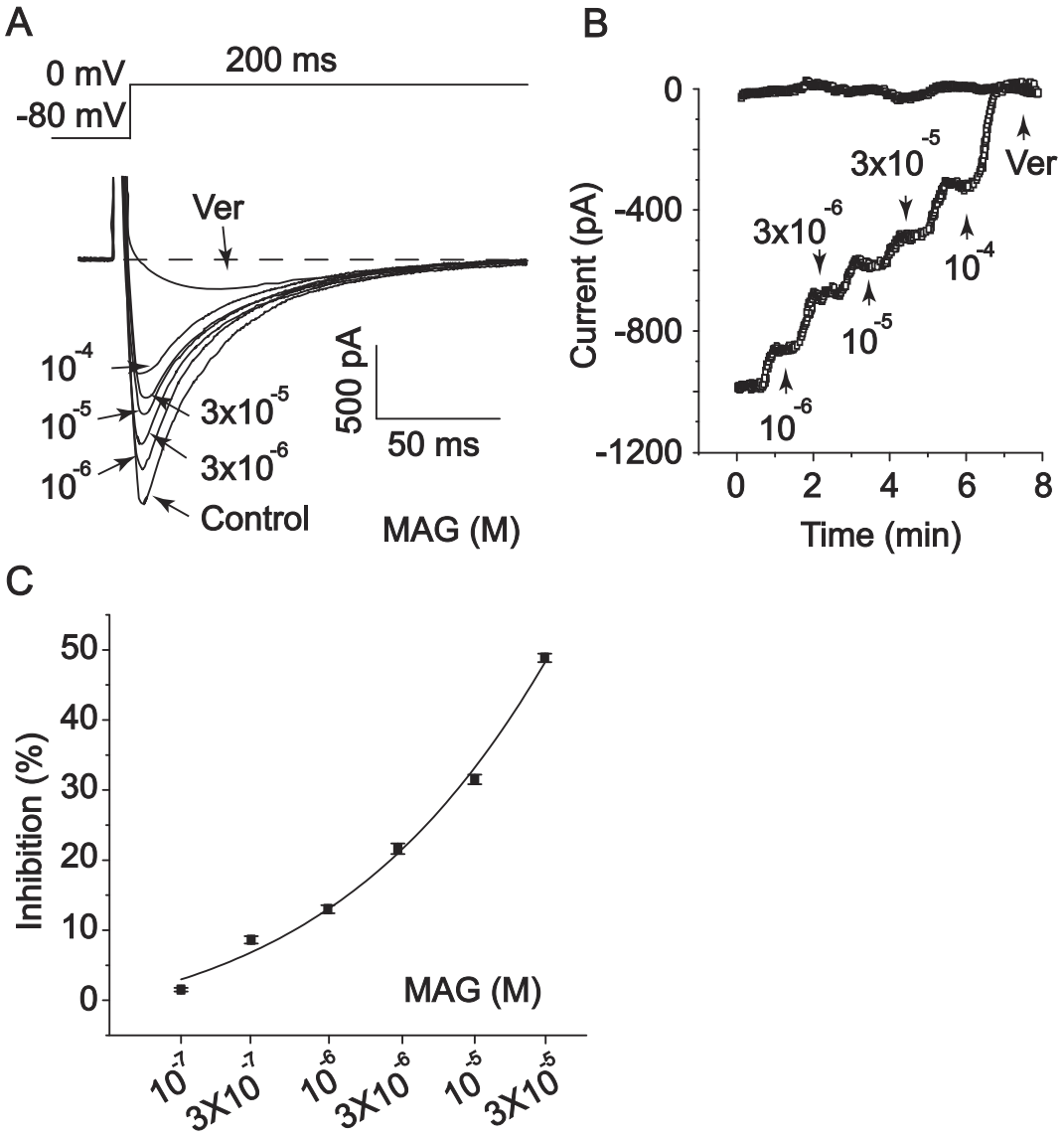

Figure 11 Actions of MAG at distinct concentrations on $I_{Ca\text{-}L}$. (**A**) Current traces of $I_{Ca\text{-}L}$ upon immerse to 1×10^{-6}, 3×10^{-6}, 1×10^{-5}, 3×10^{-5}, and 1×10^{-4} M MAG, as well as 0.1 mM Ver. (**B**) Time course of $I_{Ca\text{-}L}$ upon immersion in 1×10^{-6}, 3×10^{-6}, 1×10^{-5}, 3×10^{-5}, and 1×10^{-4} M MAG, as well as 0.1 mM Ver. (**C**) Concentration-response curve of MAG. The values are the mean ± standard deviation (n=10 cells).

includes cardiac muscle hyperactivity and intracellular calcium ion influx. Furthermore, the pathophysiology changes in the ISO-based MII model resemble the results observed in humans.[21,22]

Licorice is one of the oldest medicinal plants and contains 300 active ingredients. Licorice and its extracts have antibacterial, antiviral, anti-inflammatory, anticancer, antioxidant, and other activities. MAG is one of the important effective ingredients and has good effects in the treatment of cardiovascular disease.[23,24] It is widely used in clinical immunoregulation, the promotion of bilirubin metabolism, the suppression viral hepatitis, improvement of liver function, adjuvant therapy for tumor chemoradiotherapy, and polycystic ovary syndrome, among others.[23,24] In this study, we investigated the cardioprotective effects and possible mechanisms of MAG injection on ISO-induced MII.

ISO is a β-receptor agonist, and continuous high doses can induce myocardial infarction-like injury in experimental animals. ISO is often used in models of myocardial ischemia.[25] The literature suggests that the key factors of ischemic injury are the decrease of Ca^{2+} uptake in the sarcoplasmic reticulum of the ischemic myocardium and intracellular calcium ion influx. The myocardium is extremely sensitive to hypoxia. Hypoxia can cause intracellular calcium ion influx, which is an important mechanism that leads to myocardial cell injury and necrosis. After the intervention of

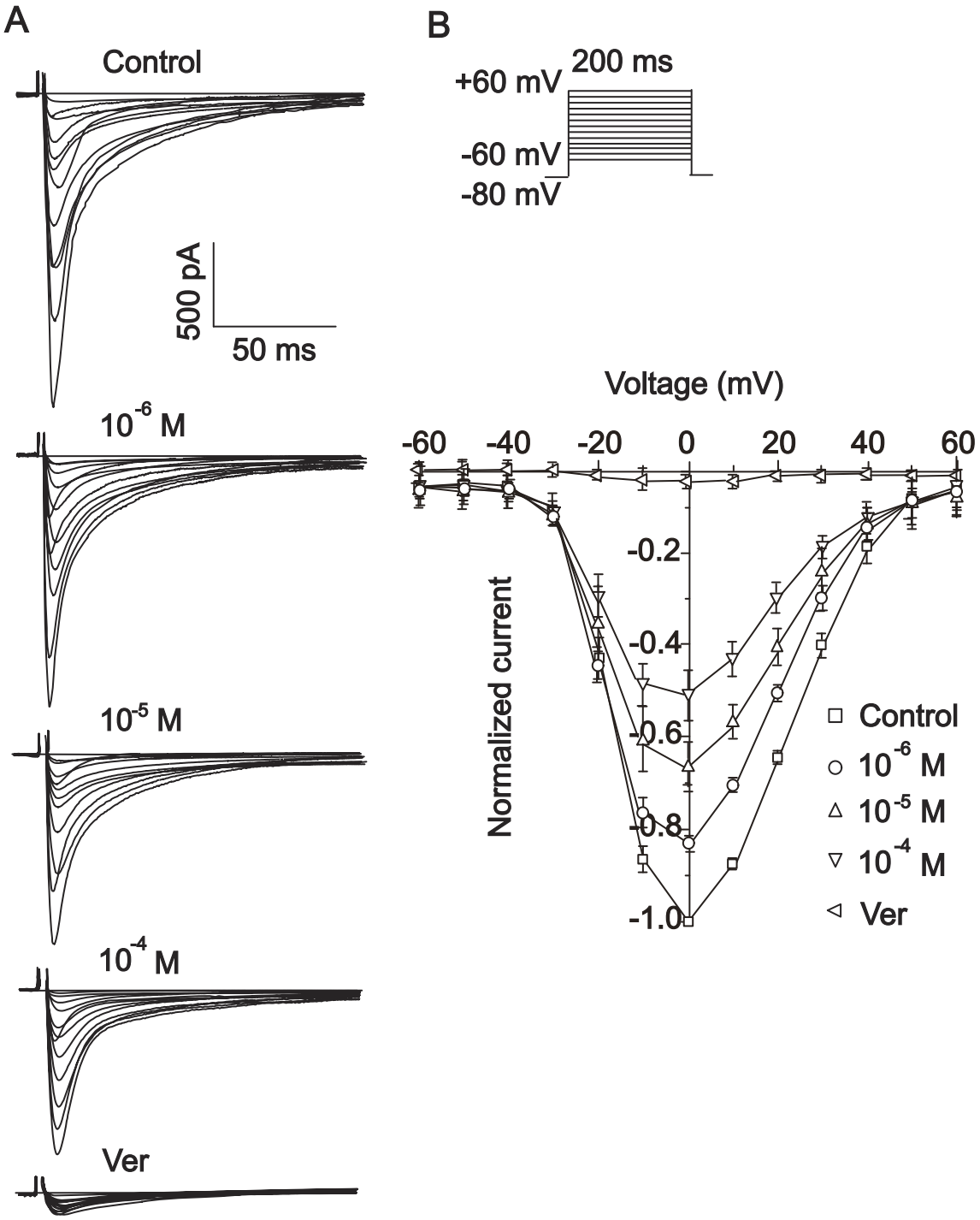

Figure 12 Actions of MAG on the I-V relationship of $I_{Ca\text{-}L}$. Example tracks (**A**) and assembled information (**B**) were obtained with the following treatments: Con (□),1×10^{-6} M MAG (○), 1×10^{-5} M MAG (△), 1×10^{-4} M MAG (▽), and 0.1 mM Ver (◁). The values are the mean ± standard deviation (n=10 cells).

MAG and Ver, the concentration of free calcium in cardiomyocytes decreased significantly (Figure 8A and B). This shows that MAG has a similar effect to that of a calcium antagonist.

Systolic and diastolic dysfunction and altered cardiac structure are some of the characteristics of an ISO-induced myocardial ischemia model. In this study, we evaluated the hemodynamic and histological changes, the decrease of LVSP and $\pm dp/dt_{max}$, the increase of LVEDP (Table 1), and the injury of myocardial tissue to confirm the effect of the ISO-induced myocardial ischemia model in rats. Under a light microscope, H&E staining sections showed that the

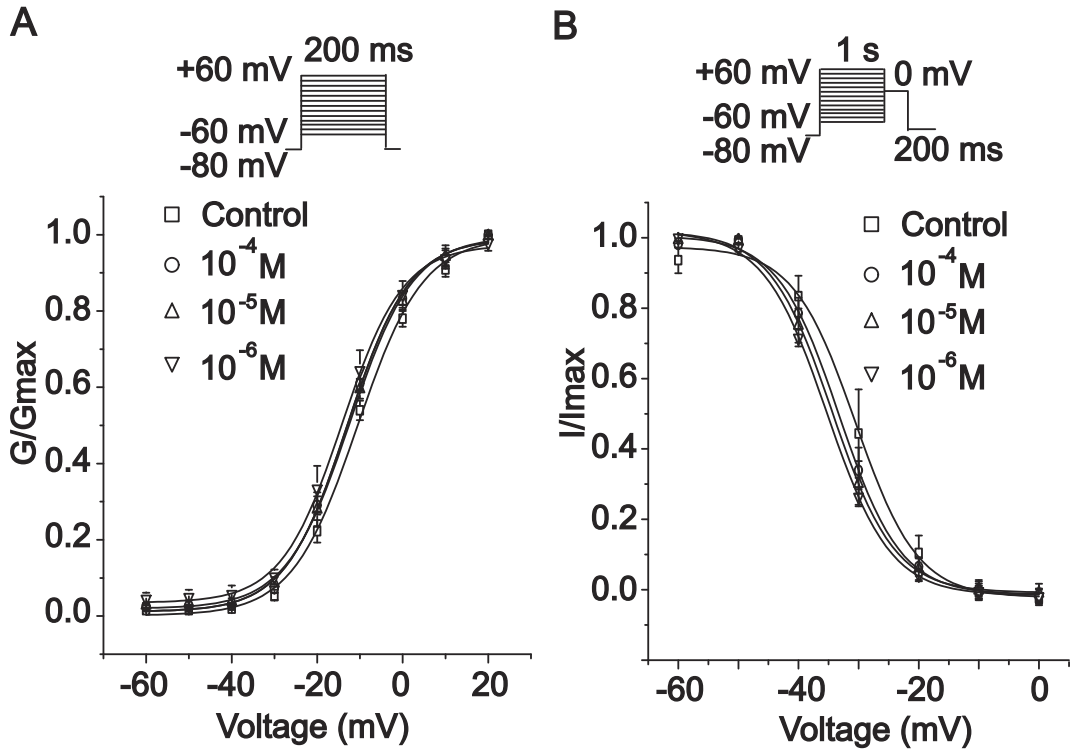

Figure 13 Actions of MAG on steady-state activation and inactivation of Ca^{2+} current. Activation dynamics (**A**) and inactivation dynamics of Ca^{2+} current (**B**) are demonstrated for the following treatments: Con (□), 1×10^{-4} M MAG (○), 1×10^{-5} M MAG (△), and MAG at 1×10^{-6} M MAG (▽). The values are the mean ± standard deviation (n=10 cells).

myocardial tissue of the ISO group was obviously damaged, the arrangement of myocardial cells was disordered, the muscle space was widened, the nucleus was pyknotic, there was deformation or dissolution, and the membrane was damaged (Figure 6A–D).

The ultrastructures of the myocardium were also observed under a light microscope. In the ISO group, some mitochondria were swollen, fused, or cristaed, and the Z-line became thinner. The MAG group and Ver group showed significantly improvements in these morphological changes (Figure 6E–H). Therefore, treatment with MAG and Ver can improve heart function.

CK and LDH are cytoplasmic enzymes that are released only in the vent of myocardial cell damage, which increases their activity. Therefore, we used CK and LDH as biochemical markers to detect cardiac cellular changes under MII conditions induced by ISO, as well as the intracellular calcium concentration. The results are shown in Figure 3. When oxidative stress is stimulated, the balance between pro-oxidation and anti-oxidation in the body tends toward pro-oxidation, which leads to homeostasis disorder along with tissue and cell damage. Oxidative stress is also one of the important reasons for the abnormal structure and function of the cardiovascular system. Oxidative stress plays a key role in the occurrence and development of cardiovascular diseases, such as atherosclerosis, myocardial ischemia-reperfusion damage, and arrhythmia.

There are many kinds of free radicals, and ROS are closely related to oxidative stress. Cells metabolize oxidants, and they have evolved enzymatic or non-enzymatic mechanisms to resist oxidant toxicity, such as myocardial and serum SOD, GSH, and MDA.[26] Often, a small amount of free radicals is produced in normal tissue metabolism, and the balance of oxygen free radicals is maintained through intracellular defense mechanisms. However, under the action of some damage factors, the oxidative metabolites in cells increase, or the antioxidant protection mechanism becomes insufficient. As a result, free radicals accumulate and produce toxic effects on cells.

This imbalance between oxidation and antioxidants is called oxidative stress. Oxidative stress directly induces the denaturation of cytosolic proteins and enzymes, apoptosis or cell death, tissue damage, and disease.[27] The scavenging mechanism of ROS includes primary and secondary antioxidant defense systems. Myocardial and serum SOD, GSH

activity, MDA content, and intracellular ROS were detected in experiments, and the results are shown in Figures 4, 5, and 7.

We tested the effects of MAG on myocardial cells and found that it reduced the calcium concentration in cardiac tissue.[28] Therefore, we used the whole-cell patch-clamp technique to investigate the effects of MAG on the intracellular conditions and ion channels. The patch-clamp results illustrate that MAG decreased $I_{Ca\text{-}L}$ in a concentration-dependent fashion, and the semi-maximal prohibitive concentration was 14 μM, as shown in Figure 11. This might have resulted from the MAG combining with the channel proteins by forming covalent bonds.[29]

The I-V relationship or $I_{Ca\text{-}L}$ reverse potential remained unchanged (Figure 12). MAG inhibited the peak value of the Ca^{2+} current without affecting the steady-state activation and inactivation of $I_{Ca\text{-}L}$ (Figure 13). The physiological process of converting an electrical stimulus to a mechanical response was characterized by excitation-contraction (EC) coupling.[30] In EC coupling, voltage-gated calcium channels are activated by membrane depolarization, and then Ca^{2+} enters the myocytes through LTCCs. Ca^{2+} entry through the nearby LTCCs then triggers the release of Ca^{2+} from ryanodine receptors.[31] The decrease of calcium results in less of a decrease in myocardial oxygen consumption, which reduces the calcium concentration in cardiac myocytes and can alleviate arrhythmia and cell damage. We found that MAG had significant but conditional inhibitory effects on $I_{Ca\text{-}L}$.

The data obtained from organs, tissues, and cells in vitro can be used to infer about the role of MAG in vivo, but our experiments in isolated cells were carried out at room temperature (25 degrees celsius). One of the limitations of this study is that there is a gap between this experimental environment and the physiological environment of cardiomyocytes. Therefore, the direct effect of MAG on $I_{Ca\text{-}L}$ needs further study.

Conclusion

We demonstrated the protective effects of MAG injection in an ISO-induced MII model. The mechanism underlying the cardioprotective effect might be related to the regulation of oxidative stress and the reduction of calcium influx by inhibiting LTCCs. These results could provide further insight into the molecular mechanisms underlying the beneficial effects of MAG injection on IHD.

Acknowledgments

This work was supported by Research Foundation of Hebei University of Chinese Medicine (No. KTZ 2019041). Zhifeng Zhao and Miaomiao Liu are co-first authors for this study.

Disclosure

The authors declare no conflicts of interest in this work.

References

1. Wang X, Zhang H, Chen L, et al. Liquorice, a unique “guide drug” of traditional Chinese medicine: a review of its role in drug interactions. *J Ethnopharmacol*. 2013;150(3):781–790. doi:10.1016/j.jep.2013.09.055
2. Fiore C, Eisenhut M, Ragazzi E, et al. A history of the therapeutic use of liquorice in Europe. *J Ethnopharmacol*. 2005;99(3):317–324. doi:10.1016/j.jep.2005.04.015
3. Rossum TGV, Vulto AG, Hop WC, et al. Intravenous glycyrrhizin for the treatment of chronic hepatitis C: a double-blind, randomized, placebo-controlled Phase I/II trial. *J Gastroenterol Hepatol*. 2010;14(11):1093–1099. doi:10.1046/j.1440-1746.1999.02008.x
4. Okamoto T. The protective effect of glycyrrhizin on anti-Fas antibody-induced hepatitis in mice. *Eur J Pharmacol*. 2000;387(2):229–232. doi:10.1016/S0014-2999(99)00807-9
5. Shiota G, Harada KI, Ishida M, et al. Inhibition of hepatocellular carcinoma by glycyrrhizin in diethylnitrosamine-treated mice. *Carcinogenesis*. 1999;20(1):59–63. doi:10.1093/carcin/20.1.59
6. Han S, Sun L, He F, et al. Anti-allergic activity of glycyrrhizic acid on IgE-mediated allergic reaction by regulation of allergy-related immune cells. *Sci Rep*. 2017;7(1):7222.
7. Zhang MF. Advances in studies on glycyrrhizic acid and its derivatives in anti-inflammation and anti-allergy. *Drugs Clin*. 2011;26(05):359–364.
8. Chen Q, Chen H, Wang W, et al. Glycyrrhetic acid, but not glycyrrhizic acid, strengthened entecavir activity by promoting its subcellular distribution in the liver via efflux inhibition. *Eur J Pharm Sci*. 2017;106:313–327. doi:10.1016/j.ejps.2017.06.015
9. Koike K. [Erratum] Expression of junB is markedly stimulated by glycyrrhizin in a human hepatoma cell line. *Oncol Rep*. 2011;25(3):609–617. doi:10.3892/or
10. Zhou L, Song Y, Zhao J, et al. Monoammonium glycyrrhizinate protects rifampicin- and isoniazid-induced hepatotoxicity via regulating the expression of transporter Mrp2, Ntcp, and Oatp1a4 in liver. *Pharm Biol*. 2016;54(6):931–937. doi:10.3109/13880209.2015.1070878
11. Wang Z, Yu J, Wu J, et al. Scutellarin protects cardiomyocyte ischemia–reperfusion injury by reducing apoptosis and oxidative stress. *Life Sci*. 2016;157:200–207. doi:10.1016/j.lfs.2016.01.018
12. Zhou S-S, He F, Chen A-H, et al. Suppression of rat Frizzled-2 attenuates hypoxia/reoxygenation-induced Ca^{2+} accumulation in rat H9c2 cells. *Exp Cell Res*. 2012;318(13):1480–1491. doi:10.1016/j.yexcr.2012.03.030
13. Andrades ME, Ritter C, Dal-Pizzol F. The role of free radicals in sepsis development. *Front Biosci (Elite Ed)*. 2009;1(1):277–287.
14. Rettie AE, Edson KZ. CYP4 enzymes as potential drug targets: focus on enzyme multiplicity, inducers and inhibitors, and therapeutic modulation of 20- Hydroxyeicosatetraenoic acid (20-HETE) synthase and fatty acid hydroxylase activities. *Curr Top Med Chem*. 2013;13(12):1429–1440. doi:10.2174/15680266113139990110
15. Nakayama H, Chen X, Baines CP, et al. Ca^{2+} and mitochondrial-dependent cardiomyocyte necrosis as a primary mediator of heart failure. *J Clin Investig*. 2007;117(9):2431–2444. doi:10.1172/JCI31060

16. Nichtova Z, Novotova M, Kralova E, et al. Morphological and functional characteristics of models of experimental myocardial injury induced by isoproterenol. *Gen Physiol Biophys*. 2012;31(2):141–151. doi:10.4149/gpb_2012_015
17. Dongworth RK, Hall AR, Burke N, et al. Targeting mitochondria for cardioprotection: examining the benefit for patients. *Future Cardiol*. 2014;10(2):255–272. doi:10.2217/fca.14.6
18. Hardy N, Viola H, Johnstone VPA, et al. Nanoparticle-Mediated dual delivery of an antioxidant and a peptide against the L-Type Ca^{2+} channel enables simultaneous reduction of cardiac ischemia-reperfusion injury. *ACS Nano*. 2015;9(1):279–289. doi:10.1021/nn5061404
19. Grynkiewicz G, Poenie M, Tsien RY. A new generation of Ca^{2+} indicators with greatly improved fluorescence properties. *J Biol Chem*. 1985;260(6):3440–3450.
20. Han X, Li M, Zhao Z, et al. Mechanisms underlying the cardioprotection of total ginsenosides against myocardial ischemia in rats in vivo and in vitro: possible involvement of L-type Ca^{2+} channels, contractility and Ca^{2+} homeostasis. *J Pharmacol Sci*. 2019;139(3):240–248. doi:10.1016/j.jphs.2019.02.001
21. Li H, Xie YH, Yang Q, et al. Cardioprotective effect of paeonol and danshensu combination on isoproterenol-induced myocardial injury in rats. *PLoS One*. 2012;7(11):e48872. doi:10.1371/journal.pone.0048872
22. Wang SB, Tian S, Yang F, et al. Cardioprotective effect of salvianolic acid A on isoproterenol-induced myocardial infarction in rats. *Eur J Pharmacol*. 2009;615(1):125–132. doi:10.1016/j.ejphar.2009.04.061
23. Sabbadin C, Bordin L, Donà G, et al. Licorice: from pseudohyperaldosteronism to therapeutic uses. *Front Endocrinol (Lausanne)*. 2019;10:484–489. doi:10.3389/fendo.2019.00484
24. Deutch MR, Grimm D, Wehland M, et al. Bioactive candy: effects of licorice on the cardiovascular system. *Foods*. 2019;8(10):pii:E495. doi:10.3390/foods8100495
25. Farvin KHS, Anandan R, Kumar SHS, et al. Effect of squalene on tissue defense system in isoproterenol-induced myocardial infarction in rats. *Pharmacol Res*. 2004;50(3):231–236. doi:10.1016/j.phrs.2004.03.004
26. Hitoshi I, Yukio K, Satoshi Y, et al. Determination of oxidative stress and cardiac dysfunction after ischemia/reperfusion injury in isolated rat hearts. *Ann Thorac Cardiovasc Surg*. 2013;19(3):186–194. doi:10.5761/atcs.oa.12.01896
27. Celes MR, Torresdueñas D, Prado CM, et al. Increased sarcolemmal permeability as an early event in experimental septic cardiomyopathy: a potential role for oxidative damage to lipids and proteins. *Shock*. 2010;33(3):322–331. doi:10.1097/SHK.0b013e3181b38ef6
28. Adams BA. Contractions of dysgenic skeletal muscle triggered by a potentiated, endogenous calcium current. *J Gen Physiol*. 1991;97(4):687–696. doi:10.1085/jgp.97.4.687
29. Du H, He J, Wang S, et al. Investigation of calcium antagonist–L-type calcium channel interactions by a vascular smooth muscle cell membrane chromatography method. *Anal Bioanal Chem*. 2010;397(5):1947–1953. doi:10.1007/s00216-010-3730-8
30. Hernández-Ochoa EO, Vanegas C, Iyer SR, et al. Alternating bipolar field stimulation identifies muscle fibers with defective excitability but maintained local Ca^{2+} signals and contraction. *Skelet Muscle*. 2015;6(1):6. doi:10.1186/s13395-016-0076-8
31. Takamatsu H, Nagao T, Ichijo H, et al. L-type Ca^{2+} channels serve as a sensor of the SR Ca^{2+} for tuning the efficacy of Ca^{2+}- induced Ca^{2+} release in rat ventricular myocytes. *J Physiol*. 2010;552(2):415–424. doi:10.1113/jphysiol.2003.050823